Aharonov-Bohm Oscillations Changed by Indirect Interdot Tunneling via Electrodes in Parallel-Coupled Vertical Double Quantum Dots

T. Hatano,[1,*] T. Kubo,[1] Y. Tokura,[1,2] S. Amaha,[1] S. Teraoka,[1] and S. Tarucha[1,3]

[1]*JST, ICORP, Quantum Spin Information Project, Atsugi-shi, Kanagawa 243-0198, Japan*

[2]*NTT Basic Research Laboratories, Atsugi-shi, Kanagawa 243-0198, Japan*

[3]*Department of Applied Physics, University of Tokyo, Hongo, Bunkyo-ku, Tokyo 113-8656, Japan*

(Received 7 January 2010; revised manuscript received 14 September 2010; published 15 February 2011)

Aharonov-Bohm (AB) oscillations are studied for a parallel-coupled vertical double quantum dot with a common source and drain electrode. We observe AB oscillations of current via a one-electron bonding state as the ground state and an antibonding state as the excited state. As the center gate voltage becomes more negative, the oscillation period is clearly halved for both the bonding and antibonding states, and the phase changes by half a period for the antibonding state. This result can be explained by a calculation that takes account of the indirect interdot coupling via the two electrodes.

DOI: 10.1103/PhysRevLett.106.076801 PACS numbers: 73.63.Kv, 73.23.Hk

Quantum coherence and the correlation of electrons in semiconductor nanostructures are of primary interest. In the past few years, they have been well characterized for qubit states in single and double quantum dots (DQDs) in the context of quantum information. Before this, the direct observation of quantum coherence in QDs had already been achieved using the Aharonov-Bohm (AB) effect [1]. The conductance or current through an AB ring oscillates periodically with the magnetic flux penetrating the ring area. For an AB ring with one quantum dot, the abrupt phase change by the half period was initially observed [2], and explained using the reciprocal theorem for a two-terminal measurement [3].

AB oscillations in current flowing through two QDs or DQDs embedded in an AB ring with one QD in each arm were studied theoretically with particular attention to the electron correlation effect [4,5]. The AB phase of a current flowing through two-electron states in a tunnel coupled DQD is predicted to be different by half a period in the cotunneling regime between the spin singlet state and triplet state due to interdot exchange coupling [6]. In contrast, for one-electron states, it is anticipated that the AB oscillations of the bonding state (BS) are phase changed by half a period from those of the antibonding state (AS), reflecting the parity of the electron wave functions in the DQD [7,8].

These features have been experimentally studied for parallel-coupled lateral DQDs [9] and vertical DQDs [10], but without reference to the phase evolution. The phase change in the AB oscillation has only recently been observed in association with inelastic cotunneling processes but unrelated to interdot coupling [11]. In all previous reports, the effect of interdot coupling was too weak to be resolved in the AB oscillations.

In this Letter, we use a laterally coupled vertical DQD to study the AB oscillations of current through the one-electron states. We first precisely identify the one-electron BS as the ground state and the AS as the excited state in the charging diagram, and then measure the AB oscillations of current through the BS and AS. We observe critical changes in the phases and periods of the AB oscillations, depending on the center gate voltages. To account for these results, we consider the effect of ''the indirect interdot tunnel coupling through the electrodes.''

Our device consists of laterally coupled vertical DQDs with four split gates made from a double-barrier heterostructure (see supplementary material [12]) [13,14].

It is usually assumed that electron coherence readily collapses in the electrodes. However, this was not the case in our previous experiment on the same type of DQD device as used here because AB oscillations were indeed observed for the AB ring encircled through the source and drain [10]. This is because the electrodes are adjacent to the thin AlGaAs tunnel barriers just outside the QDs. Therefore, we assume for the vertical QDs that the two QDs are coupled via the n-AlGaAs contact layers in a sufficiently short path length to maintain the coherence. Here, we introduce the indirect interdot tunnel coupling parameter α_s and α_d ($|\alpha_{s(d)}| \leq 1$), which indicates the degree of coherence in the source and drain, respectively [8]. When $\alpha_{s(d)} = 0$, the coherence is completely lost; the AB oscillation is not observed. In contrast, the coherence in the electrodes is completely conserved at $|\alpha_{s(d)}| = 1$; the visibility of the AB oscillation is at its maximum. Note that the visibility of the AB oscillation is 100% when the energy level in each dot is aligned. In actual systems, however, such a $|\alpha_{s(d)}| = 1$ case is very special and most experimental situations correspond to $|\alpha_{s(d)}| < 1$. In particular, in the measured device, we assume $|\alpha_{s(d)}| \lesssim 0.2$, as described below [12].

Then two current loops with more or less the same area, $S/2$, are formed due to the presence of the direct interdot tunnel coupling. The magnetic flux, which penetrates the large current loop of the area S, including the two small

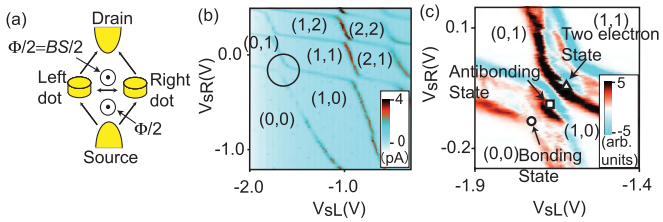

FIG. 1 (color). (a) Diagram of current flow (I_{SD}) in parallel-coupled double quantum dot. The arrows indicate the current flow. (b) Color plot of I_{SD} as a function of the left and right side gate voltages, V_{sL} and V_{sR}, at a source drain voltage $V_{SD} = 50\ \mu$V and a center gate voltage $V_c = -1.20$ V. (N_L, N_R) denotes the electron numbers in the left and right dots. (c) Color plots of the average values of the transconductance $(dI_{SD}/dV_{sL} + dI_{SD}/dV_{sR})/\sqrt{2}$ as a function of V_{sL} and V_{sR} at $V_c = -1.20$ V and $V_{SD} = 800\ \mu$V, corresponding to the region within the circle in (b).

same-sized loops, is defined by $\Phi = BS$, as shown in Fig. 1(a), where B is an externally applied in-plane magnetic field. Thus, the magnetic flux, which penetrates each small loop, is $\Phi/2$. The evaluated AB oscillation period is $\Delta B_0 = 2\Phi_0/S = 0.77$ T, where $\Phi_0 = h/e$ is the magnetic flux quantum, h is the Planck constant, and e the electron charge [12]. All the transport measurements are performed on a device placed in a dilution refrigerator with a base temperature of 20 mK.

Figure 1(b) shows current (I_{SD}) peaks or Coulomb peaks evolving with left and right gate voltages, V_{sL} and V_{sR}, measured at a bias voltage, $V_{SD} = 50\ \mu$V. The center gate voltage, V_c, is fixed at -1.20 V. No Coulomb peaks are observed for $V_{sL} \lesssim -1.7$ V and $V_{sR} \lesssim -0.1$ V, indicating that the DQD is empty. Then, the electron number $N_L(N_R)$ in the left (right) QD increases by one whenever the point in the parameter space in Fig. 1(b) crosses one of the Coulomb peaks on the right (top). Therefore, the charge states with (N_L, N_R) are fixed in each hexagon formed by the Coulomb peaks.

Figure 1(c) shows the average value of the transconductance $(dI_{SD}/dV_{sL} + dI_{SD}/dV_{sR})/\sqrt{2}$ as a function of V_{sL} and V_{sR} at $V_c = -1.20$ V and $V_{SD} = 800\ \mu$V. The two anticrossing stripes indicate that the Coulomb peaks are widened by applying a finite V_{SD}. The lower left and upper right stripes correspond to the one- and two-electron states, respectively. The red or black lower border line of each stripe indicates the ground state, and the red or black line inside the lower left stripe is the one-electron excited state [14]. For the one-electron stripe, we observe that the ground and excited states anticross with each other as a typical feature of the resonance between the BS and AS, which are indicated by the circle and square in Fig. 1(c), respectively [14]. We estimated an interdot tunnel coupling $2t$ of 0.53 meV. The interdot Coulomb coupling energy V_{inter} is approximately 0.4 meV. The tunneling rates from the source and drain electrodes to the DQD, Γ_s and Γ_d, are estimated to be $\sim$0.5 and $\sim$1.5 μeV, respectively.

For the two-electron state, the excited state is not well resolved in Fig. 1(c), probably because the exchange coupling energy that corresponds to the energy separation between the singlet and triplet states is very small [14]. Therefore, the state indicated by the triangle is the two-electron ground state.

We measured the current at the circle and square points as a function of B for various V_c values. The two points are defined by the charging diagram measurement at $B = 0$ T (not shown). Here, let us consider the BS and AS currents. The current at the circle in Fig. 1(c) flows solely through the BS because only the BS is within the bias window, which is caused by applying V_{SD}. Consequently, the current is the BS current. On the other hand, at the square the current flows through the BS and AS, since both states are in the bias window. Using the BS and AS as the bases, the diagonal elements of a transmission matrix indicate the transmission probabilities of the BS and AS, and the total current is calculated by integrating the transmission probabilities in the bias window with respect to energy [12,15]. Moreover, the current flowing through the system generally accompanies the mixing component of the BS and AS currents, which corresponds to the higher order tunneling processes comprising both BS and AS. However, these processes, which are proportional to the second order terms of $\alpha_{s(d)}$, can be neglected, since $\alpha_{s(d)}$ is very small in our case [12]. Therefore, we can simply describe the total current as the sum of the BS and AS currents. Then, we can assume that the BS currents at the circle and square are almost the same, because the potential barrier height, i.e., the electron transmission probability, at the circle and square hardly changes. Consequently, we subtracted the current measured for the BS from that at the square to extract the AS current.

The currents obtained for the BS and AS are shown as a function of B in Figs. 2(a) and 2(b), respectively, where V_{SD} and V_c are the same as those in Fig. 1(c). Both currents oscillate periodically with B; these oscillations are AB oscillations. The fast Fourier transform (FFT) spectra of 2(a) and 2(b) in the insets show peaks at 0.81, and 0.79 T, respectively. These values are consistent with the calculated value of $\Delta B_0 = 0.77$ T. Therefore, this oscillation corresponds to area $S/2$ rather than area S owing to direct interdot tunnel coupling [7,8]. There is a good half period contrast between 2(a) and 2(b) because there is a current dip at $B = 0$ T for BS whereas there is a peak for AS. Note that the small dip at around ± 1 T in Fig. 2(b) is probably because the contribution of the BS current is not completely subtracted in the derivation of the AS current.

The BS and AS currents obtained for $V_c = -1.26$, -1.36, and -1.40 V and at $V_{SD} = 700$, 500, and 500 μV are shown in Figs. 2(c)–2(h), respectively. Here $2t$ is estimated to be 0.46, 0.35, and 0.24 meV at $V_c = -1.26$, -1.36, and -1.40 V, respectively. The interdot Coulomb coupling energy V_{inter} is approximately 0.4 meV for the three different V_c values. In Figs. 2(c)

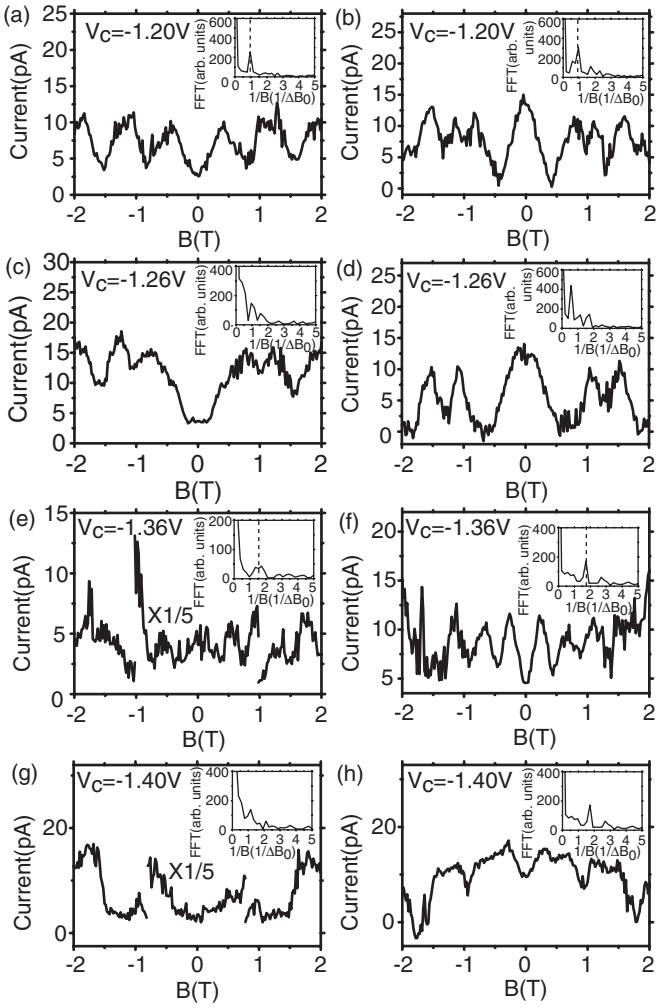

FIG. 2. Current flowing through the bonding state (a),(c),(e), (g) and the antibonding state (b),(d),(f),(h) as a function of B for $V_c = -1.20$, -1.26, -1.36, and -1.40 V and at $V_{\mathrm{SD}} = 800$, 700, 500, and 500 μV, respectively. Each inset shows the corresponding fast Fourier transform (FFT) spectrum of the current oscillation, where $\Delta B_0 = 2\Phi_0/S = 0.77$ T.

and 2(d) at $V_c = -1.26$ V, the current oscillations are not very periodic, but on the whole they are similar to those in Figs. 2(a) and 2(b), respectively. The FFT spectrum in Fig. 2(d) shows that the largest peak is slightly different from that in Fig. 2(b), reflecting the larger peak spacing at $B = 0$ and ± 1.1 T.

The currents obtained for the more negative V_c values show markedly different features. At $V_c = -1.36$ V, the BS current oscillates only weakly with B in Fig. 2(e). The oscillation period of 0.5 T as identified in the FFT spectrum is approximately half the value obtained for the BS current at $V_c = -1.20$ V 2(a) and -1.26 V 2(c). In contrast, for the AS current in Fig. 2(f), we observe clear oscillations with a period of 0.44 T, which is almost the same as that for the BS current in 2(e). The AB oscillation of the AS current in 2(f) with $V_c = -1.36$ V has a dip at $B = 0$ T, whereas it has a peak at $V_c = -1.20$ V 2(b) and $V_c = -1.26$ V 2(d). On the other hand, that of the BS current in 2(e) for $V_c = -1.36$ V seems to leave a small peak at $B = 0$ T, judging from the magnified plot. However, because the BS current is smaller than 1 pA for $|B| < 1$ T and comparable to the noise level, it is difficult to resolve the AB oscillation at around $B = 0$ T.

The AB oscillations are significantly damped for both BS and AS when V_c becomes even more negative at -1.40 V in Figs. 2(g) and 2(h). The features of the AB oscillations appear similar to those at $V_c = -1.36$ V, although the AB oscillation of the BS is not very clear. The application of a more negative voltage to the center gate voltage weakens the direct interdot tunnel coupling. Moreover, it increases the dephasing in the electrodes because of the increase in the effective path length in the electrode to connect the two dots. The latter could be the reason for the reduced visibility of the AB oscillations at $V_c = -1.36$ and -1.40 V in Figs. 2(e)–2(h).

However, possible changes in the distance between the two dots and the direct interdot tunnel coupling and in the dephasing caused by applying a much more negative V_c cannot account for either the abrupt changes in the phase or the period of AB oscillations with V_c as observed in Fig. 2. Here, we consider that the interference effect induced by the indirect interdot tunnel coupling via the electrodes [12] accounts for the observed features.

First, let us simply analyze the currents flowing through the BS and AS, when the bias voltage is so large that the BS and AS are in the bias window. We define the tunneling rate $\Gamma_{bb}^{S(D)}$ through the BS and $\Gamma_{aa}^{S(D)}$ through the AS from the source (drain) electrode to the DQD. They are described as [8]

$$\Gamma_{bb}^{S(D)} = \Gamma_{s(d)}\{1 + \alpha_{s(d)} \cos(\pi\Phi/\Phi_0)\}, \quad (1)$$

$$\Gamma_{aa}^{S(D)} = \Gamma_{s(d)}\{1 - \alpha_{s(d)} \cos(\pi\Phi/\Phi_0)\}, \quad (2)$$

where $\Gamma_{s(d)}$ corresponds to the tunneling rate from the source (drain) electrode to the DQD at $\alpha_s = \alpha_d = 0$; otherwise, the $\alpha_{s(d)}$ parameters are assumed to be the same between the BS and AS. Because the higher order tunneling processes comprising both the BS and AS can be neglected due to the small $\alpha_{s(d)}$ in our case as explained above, the currents, I_b through the BS and I_a through the AS, are expressed as

$$I_{b(a)} \propto (1/\Gamma_{bb(aa)}^{S} + 1/\Gamma_{bb(aa)}^{D})^{-1}, \quad (3)$$

respectively [12]. When α_s and α_d have the same sign, I_b (I_a) directly reflects the oscillatory parts in Γ_{bb}^{S} and Γ_{bb}^{D} (Γ_{aa}^{S} and Γ_{aa}^{D}) with the same period of $2\Phi_0$ in phase. Then, as expected from Eqs. (1) and (2), the AB oscillation phase is different by a half period, i.e., Φ_0, between I_b and I_a. On the other hand, when α_s and α_d have opposite signs, the oscillation amplitude of I_b (I_a) becomes small because Γ_{bb}^{S} and Γ_{bb}^{D} (Γ_{aa}^{S} and Γ_{aa}^{D}) oscillate with the same period of $2\Phi_0$ but in the opposite phase. Consequently, the AB oscillations of I_b and I_a appear to

be in phase with the period of $2\Phi_0$ but with an extra dip or peak, although the visibility of the AB oscillations should be lower than that when α_s and α_d have the same sign. Therefore, it is possible to account for the changes in the period and phase of the AB oscillation with respect to V_c by using $\alpha_{s(d)}$.

Here, let us discuss the experimental result in Fig. 2 concretely, using the change of $\alpha_{s(d)}$. Initially, we consider the signs of α_s and α_d at $V_c = -1.20$ V in our experiment. The phases of the AB oscillations for the BS and the AS in Figs. 2(a) and 2(b) are not consistent with those predicted for $\alpha_s = \alpha_d = 1$ [7]. This discrepancy can be explained by assuming that both α_s and α_d have negative signs. Then, we consider the changes in α_s and α_d as V_c becomes more negative. $\alpha_{s(d)}$ decreases to 0 with oscillation as the path length in the source (drain) electrode increases [12]. α_d probably depends on the change in V_c more strongly than α_s, because the screening effect is stronger in the drain than in the source in the side of the substrate. Therefore, for simplicity we assume that α_s remains a negative constant as $\alpha_s = -0.1$ and that α_d changes from negative to positive, i.e., $\alpha_d = -0.2$ to 0.2 then to 0.15, and we calculate the currents flowing through the BS and AS numerically using the nonequilibrium Green function method. The results are shown in Figs. 3(a)–3(c). We used $2t/\hbar\Gamma = -265$ and $eV_{\mathrm{SD}}/\hbar\Gamma = 400$ in 3(a), $2t/\hbar\Gamma = -175$ and $eV_{\mathrm{SD}}/\hbar\Gamma = 250$ in 3(b), and $2t/\hbar\Gamma = -120$ and $eV_{\mathrm{SD}}/\hbar\Gamma = 250$ in 3(c), with $V_{\mathrm{inter}}/\hbar\Gamma = 200$, $k_BT/\hbar\Gamma = 10$ as common parameters, where k_B is the Boltzmann constant, T is the temperature, $\hbar = h/2\pi$ and $\Gamma = \Gamma_s + \Gamma_d$ ($\Gamma_s = 0.3\Gamma$ and $\Gamma_d = 0.7\Gamma$), respectively. We evaluated all these parameters experimentally.

Figure 3(a) shows AB oscillations with the same period of $2\Phi_0$ but misaligned by Φ_0 between the BS and AS, so that the BS and AS currents have a dip and a peak at $\Phi = 0$, respectively. These features are consistent with those at $V_c = -1.20$ V in Figs. 2(a) and 2(b). When α_d becomes 0.2, which corresponds to the more negative V_c [12], Fig. 3(b) shows almost the same AB oscillations with a period Φ_0 for both BS and AS; the period of the AB oscillation changes. Furthermore, the AS current at $\Phi = 0$ in 3(b) is a dip, while it is a peak in Fig. 3(a); the phase of the AB oscillation of the AS current also changes. These features are comparable to those in Figs. 2(e) and 2(f)

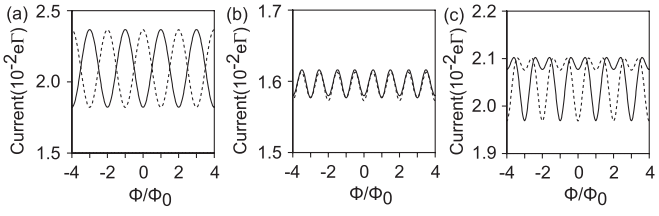

FIG. 3. Currents flowing through the bonding (solid line) and antibonding (dashed line) states as a function of magnetic flux Φ at (a) $\alpha_s = -0.1$ and $\alpha_d = -0.2$, (b) $\alpha_s = -0.1$ and $\alpha_d = 0.2$, and (c) $\alpha_s = -0.1$ and $\alpha_d = 0.15$, where $\Gamma = \Gamma_s + \Gamma_d$.

($V_c = -1.36$ V). When α_d becomes 0.15, which corresponds to a more negative V_c, Fig. 3(c) also shows AB oscillations with a period $2\Phi_0$ for both BS and AS but with an extra small dip. This feature is similar to that for the AS current in Fig. 2(h) at $V_c = -1.40$ V, although the AB oscillation for the BS current is not clear in Fig. 2(g). Regarding Figs. 2(c) and 2(d), because $V_c = -1.26$ V is an intermediate point between $V_c = -1.20$ and -1.36 V, α_d probably represents the change from negative to positive. Therefore, the AB oscillations of the BS and AS are not as clear as those at $V_c = -1.20$ V because of the small absolute value of α_d. Note that the small dip in the AS current at $\Phi = 0$ in Fig. 1(d) probably evolves into the large dip in Fig. 1(f).

The AB oscillations of the BS are not as clear as those of the AS in Figs. 2(e)–2(h). We do not fully understand the reason for this, but consider that the $\Gamma_{s(d)}$ value of the BS is smaller than that of the AS at around $\Phi \approx 0$ when $\alpha_{s(d)}$ is negative [see Eqs. (1) and (2)], resulting in the smaller BS current at around zero magnetic field.

In conclusion, we have investigated AB oscillation for the BS and AS in a DQD. The periods of the AB oscillations are roughly halved and, for the AS, the AB phase shifts by Φ_0, depending on the center gate voltage. These features are assigned to contributions from indirect interdot tunnel coupling, which depends on the center gate voltage.

Part of this work is financially supported by JSPS Grant-in-Aid for Scientific Research S (No. 19104007), MEXT Grant-in-Aid for Scientific Research on Innovative Areas (21102003), Funding Program for World-Leading Innovative R&D on Science and Technology(FIRST), and IARPA Grant No. W911NS-10-1-0330.

*hatano@ncspin.jst.go.jp

[1] Y. Aharonov and D. Bohm, Phys. Rev. **115**, 485 (1959).
[2] A. Yacoby *et al.*, Phys. Rev. Lett. **74**, 4047 (1995).
[3] A. Levy Yeyati and M. Büttiker, Phys. Rev. B **52**, R14 360 (1995).
[4] H. Akera, Phys. Rev. B **47**, 6835 (1993).
[5] W. Izumida, O. Sakai, and Y. Shimizu, J. Phys. Soc. Jpn. **66**, 717 (1997).
[6] D. Loss and E. V. Sukhorukov, Phys. Rev. Lett. **84**, 1035 (2000).
[7] K. Kang and S. Y. Cho, J. Phys. Condens. Matter **16**, 117 (2004).
[8] T. Kubo *et al.*, Phys. Rev. B **74**, 205310 (2006).
[9] A. W. Holleitner *et al.*, Phys. Rev. Lett. **87**, 256802 (2001).
[10] T. Hatano *et al.*, Physica (Amsterdam) **22E**, 534 (2004).
[11] M. Sigrist *et al.*, Phys. Rev. Lett. **96**, 036804 (2006).
[12] See supplemental material at http://link.aps.org/supplemental/10.1103/PhysRevLett.106.076801 for auxiliary explanation.
[13] T. Hatano, M. Stopa, and S. Tarucha, Science **309**, 268 (2005).
[14] T. Hatano *et al.*, Phys. Rev. B **77**, 241301(R) (2008).
[15] Y. Meir and N. S. Wingreen, Phys. Rev. Lett. **68**, 2512 (1992).